J. Fluid Mech. (1967), *vol.* 27, *part* 1, *pp.* 155–175
Printed in Great Britain

Vortex decay above a stationary boundary

By ALBERT I. BARCILON
Engineering Sciences Laboratory, Harvard University†

(Received 13 January 1966 and in revised form 10 May 1966)

An attempt is made to understand the decay of a free vortex normal to a stationary, infinite boundary. For rapidly swirling flows in fluids of small viscosity, thin boundary layers develop along the rigid boundary and along the axis, the axial boundary layer being strongly influenced by the behaviour of the plate boundary. An over-all picture of the flow is sought, with only moderate success in the region far from the origin. Near the origin, the eruption of the plate boundary layer into the axial boundary layer is studied.

1. Introduction

The mathematical flow to be investigated has some features in common with the decay of strong atmospheric vortices like the dust-devil or the tornado, despite the fact that we shall consider the flow to be laminar and the fluid incompressible, and that thermal effects will not be taken into consideration. In what follows we shall study the decay for $t > 0$ of a potential swirling flow when, at $t = 0$, we suddenly impose a constant positive value ν to the kinematic viscosity. The flow prevailing at $t = 0$ is taken to be a potential vortex, found in a body of fluid bounded by $0 \leqslant r, z \leqslant \infty$ and swirling on top of an infinite stationary horizontal plate located at $z = 0$, the vortex line being coincident with the z-axis. The strength of the circulation of the semi-infinite vortex line is $\Gamma_\infty = 2\pi A_\infty$, where A_∞ denotes the initial angular momentum of all fluid particles. To complete our mathematical model, we shall assume that the fluid has a constant density ρ' and that the flow is axially symmetric.

In the initial potential flow, a fluid particle describes with no spin a circular orbit centred on the vortex line taken to be coincident with the z-axis. The only two forces acting on such a particle are a radial pressure gradient and a centrifugal acceleration. These two radial forces are equal and opposite: No meridional motion is present. Aside from the vortex line and vortex sheet found on top of the plate, the bulk of the flow has no vorticity. At $t = 0$, as the kinematic viscosity switches from zero to ν, the vortex line and vortex sheet will be smeared out and vorticity diffuses, from the plate and from the axis, into the fluid. The no-slip condition at the plate decelerates fluid particles near it and thus destroys the radial balance of forces acting on a fluid particle. As a result, the unbalanced radial pressure gradient drives fluid inward in a layer above the plate. The

† Present affiliations: Department of Meteorology, Massachusetts Institute of Technology and Department of Meteorology at Harvard University.

thickness of this layer is of the order of $\sqrt{(\nu t)}$. The fluid moving inward in the plate boundary layer erupts at the origin and rises axially in an axial 'boundary layer'. It eventually returns to the inviscid region, thus generating a vertical circulation cell. Vorticity is then redistributed by diffusion and by convection. Figure 1 illustrates the regions of a meridional plane in the physical space where these mechanisms are present. Far from the origin the governing equations are linear: vorticity is primarily redistributed by a diffusive mechanism. Near the origin, the convective redistribution of vorticity becomes important and the governing equations are non-linear. We shall devise some approximate methods to deal with these equations.

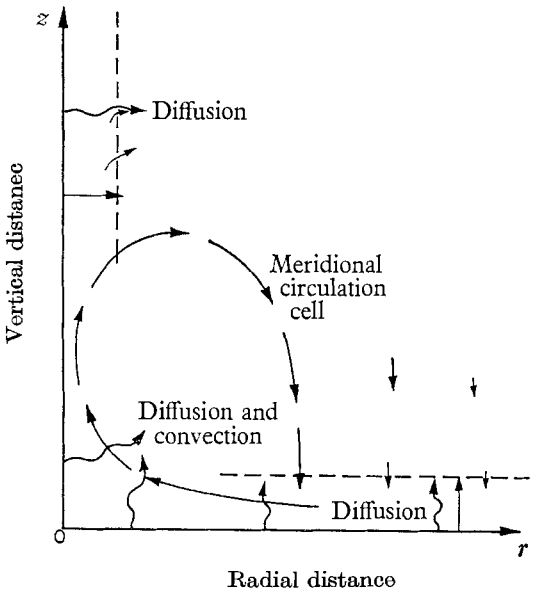

FIGURE 1. Dominant mechanisms for the redistribution of vorticity in the physical plane.

2. Formulation of the problem

If we denote by $\mathbf{v}'$ the dimensional velocity vector and by $\boldsymbol{\omega}'$ the vorticity vector $\nabla' \times \mathbf{v}'$, we can write the governing equations as (cf. Goldstein 1960, p. 89)

$$\frac{\partial \mathbf{v}'}{\partial t} + \boldsymbol{\omega}' \times \mathbf{v}' + \nabla' \left(\frac{p'}{\rho'} + \tfrac{1}{2}\mathbf{v}'^2 \right) = -\nu \nabla' \times (\nabla' \times \mathbf{v}'), \tag{1}$$

and

$$\nabla' . \mathbf{v}' = 0, \tag{2}$$

where p' and ρ' are the pressure and the constant density and where a prime denotes dimensional operators and dimensional dependent functions. The only two parameters at our disposal are the initial angular momentum A_∞ and the kinematic viscosity ν. Both these parameters have the same dimensions and

therefore, using $\sqrt{(A_\infty t)}$ as a characteristic length, we can define the following dimensionless functions:

$$\left.\begin{aligned} \mathbf{v}(\mathbf{R};\epsilon) &= \frac{\sqrt{(A_\infty t)}}{A_\infty}\mathbf{v}', \quad p(\mathbf{R};\epsilon) = \frac{t}{A_\infty}\left(\frac{p'}{\rho'}\right), \\ \boldsymbol{\omega}(\mathbf{R};\epsilon) &= t\boldsymbol{\omega}', \quad A(\mathbf{R};\epsilon) = A'/A_\infty, \end{aligned}\right\} \tag{3}$$

where

$$\epsilon = \nu/A_\infty; \tag{4}$$

the vector $\mathbf{R}$ is a dimensionless vector having cylindrical components (ξ, η) contained in the meridional plane. The new independent variables ξ and η are defined as

$$\xi = r/\sqrt{(A_\infty t)}, \quad \eta = z/\sqrt{(A_\infty t)},$$

where (r, z) is the dimensional cylindrical system having the initial vortex line as the z-axis and the plate as the $(z = 0)$-plane. Let us also introduce spherical co-ordinates (R, θ) where θ is the colatitude; the dimensionless spherical radius R is defined as

$$R = |\mathbf{R}| = \rho/\sqrt{(A_\infty t)},$$

where ρ is the dimensional spherical radius. The meridional plane containing the $\mathbf{R}$ vector will be called the $(\mathbf{R})$-plane or the mathematical plane. In this plane, the streamlines are the image of the streamlines found, at any instant, in a physical meridional plane. The $(\mathbf{R})$-plane streamlines are stationary. For $\epsilon \ll 1$, we divide the $(\mathbf{R})$-plane into: a plate boundary-layer region, an axial boundary-layer region, a corner region linking the previously mentioned regions and an inviscid region. In the inviscid region, viscous forces are small compared with inertial forces and can be neglected.

The reduction from three independent variables (r, z, t) to two independent variables (ξ, η) or (R, θ) makes it convenient to formulate the problem in the $(\mathbf{R})$-plane. When we substitute (3) and (4) into (1) and (2) we obtain

$$-\tfrac{1}{2}[\mathbf{v} + (\mathbf{R}.\boldsymbol{\nabla})\,\mathbf{v}] + \boldsymbol{\omega} \times \mathbf{v} + \boldsymbol{\nabla}(p + \tfrac{1}{2}\mathbf{v}^2) = -\epsilon\boldsymbol{\nabla} \times (\boldsymbol{\nabla} \times \mathbf{v}), \tag{5}$$

and

$$\boldsymbol{\nabla}.\mathbf{v} = 0, \tag{6}$$

where the unprimed operators are equal to $(A_\infty t)^{-\frac{1}{2}}$ times the primed operators. As boundary conditions we demand that for $\xi \sim O(\sqrt{\epsilon})$, $\eta = \infty$:

$$u = w = 0, \quad A = \xi v = 1 - \exp(-\xi^2/4\epsilon), \tag{7}$$

for $(\xi^2 + \eta^2) \to \infty$, $\xi \neq \eta \neq 0$:

$$u = w = 0, \quad A = \xi v = 1, \tag{8}$$

for $\xi = \infty$, $\eta \sim O(\sqrt{\xi})$:

$$u = w = 0, \quad A = \xi v = \exp(\tfrac{1}{2}\eta\sqrt{\epsilon}), \tag{9}$$

where (u, v, w) are the components of $\mathbf{v}$ along increasing (ξ, ψ, η) where ψ is the azimuthal angle. The boundary conditions (7) are identical with those for the diffusion of an infinite vortex line with circulation Γ_∞; i.e. we anticipate that, near the axis and at large distances from the origin, the flow will not be affected by the plate. Similarly, the boundary conditions (9) assert that near $\xi = \infty$ the flow resembles the diffusion of a vortex sheet of strength A_∞/ξ. We have transformed the problem from an initial-value problem to a boundary-value problem: the

initial condition becomes the boundary condition on the arc $0 < \theta < \frac{1}{2}\pi$, $R = \infty$. The requirement that $u = w = 0$ on that arc is consistent with the initial potential vortex flow.

On the plate, the no-slip condition demands that for $\xi > 0$, $\eta = 0$

$$u = v = w = 0, \tag{10}$$

while on the axis we impose the condition

$$u = v = \partial w/\partial \xi = 0. \tag{11}$$

Since $w = 0$ on the plate, $\partial w/\partial \xi$ is also zero on that boundary and thus there is no jump in the boundary values found along the axis and along the plate. Also, the boundary conditions on the axis, at $\eta = \infty$, and along the plate, at $\xi = \infty$, merge with those found on the arc $0 < \theta < \frac{1}{2}\pi$, $R = \infty$.

3. Plate boundary-layer solution for large values of ξ

Denote by Ψ the Stokes stream function defined as

$$\xi u = \Psi_\eta \quad \text{and} \quad \xi w = -\Psi_\xi, \tag{12}$$

and introduce the function $\phi(\xi, \eta; \epsilon)$ related to Ψ through the relation

$$\phi(\xi, \eta; \epsilon) = \xi^2 \Psi(\xi, \eta; \epsilon). \tag{13}$$

Anticipate the plate boundary-layer thickness to be of the order of $\sqrt{\epsilon}$ and define the stretched co-ordinate ζ as

$$\zeta = \eta/\sqrt{\epsilon}. \tag{14}$$

The unbalanced radial pressure gradient is the driving force in the radial momentum equation and such a force is $O(\epsilon^0)$. Therefore, we anticipate that $u \sim v \sim O(\epsilon^0)$ and that $\phi \sim O(\sqrt{\epsilon})$. We shall also assume $\partial/\partial\xi \ll \partial/\partial\eta$, which is consistent with the requirement that the boundary layer is thin; at a given station ξ, the pressure does not vary appreciably across the boundary layer and can be equated to the pressure in the inviscid flow at that station. Define the ϵ-expansions for ϕ and A as

$$\phi(\xi, \eta; \epsilon) = \epsilon^{\frac{1}{2}}\phi^{(0)}(\xi, \zeta) + \epsilon\phi^{(1)}(\xi, \zeta) + \ldots, \tag{15}$$

and

$$A(\xi, \eta; \epsilon) = A^{(0)}(\xi, \zeta) + \epsilon^{\frac{1}{2}}A^{(1)}(\xi, \zeta) + \ldots. \tag{16}$$

To obtain the governing plate boundary-layer equations, substitute (12), (13), (14), (15) and (16) into the cylindrical equations of motion and retain terms of order (ϵ^0). The resulting equations read:

radial momentum equation

$$\underbrace{\phi^{(0)}_{\zeta\zeta\zeta}}_{1} + \underbrace{(\tfrac{1}{2}\zeta\phi^{(0)}_{\zeta\zeta} + \tfrac{1}{2}\xi\phi^{(0)}_{\xi\zeta} - \phi^{(0)}_{\zeta})}_{2} - \underbrace{(1 - A^{(0)^2})}_{3} = \underbrace{(1/\xi^4)(2\phi^{(0)}\phi^{(0)}_{\zeta\zeta} - 3\phi^{(0)^2}_{\zeta}) + (1/\xi^3)(\phi^{(0)}_{\xi\zeta}\phi^{(0)}_{\zeta} - \phi^{(0)}_{\xi}\phi^{(0)}_{\zeta\zeta})}_{4}; \tag{17}$$

and angular momentum equation

$$\underbrace{A^{(0)}_{\zeta\zeta}}_{a} + \underbrace{(\tfrac{1}{2}\xi A^{(0)}_{\xi} + \tfrac{1}{2}\zeta A^{(0)}_{\zeta})}_{b} = \underbrace{(2\phi^{(0)}A^{(0)}/\xi^4) + (1/\xi^3)(\phi^{(0)}_{\zeta}A^{(0)}_{\xi} - \phi^{(0)}_{\xi}A^{(0)}_{\zeta})}_{c}; \tag{18}$$

with $$\phi^{(0)}(\xi, 0) = \phi_\xi^{(0)}(\xi, 0) = \phi_\xi^{(0)}(\xi, \infty) = 0, \tag{19}$$

and $$A^{(0)}(\xi, 0) = 0, \quad A^{(0)}(\xi, \infty) = 1, \quad A^{(0)}(\infty, \zeta) = \operatorname{erf}(\tfrac{1}{2}\zeta). \tag{20}$$

In the above equations –1– and –*a*– measure the viscous forces, –2– and –*b*– represent the local accelerations, –3– is the difference between the radial pressure gradient and the centrifugal acceleration, while –4– and –*c*– measure the convective accelerations. For $\xi \gg 1$, the local accelerations will outweigh the

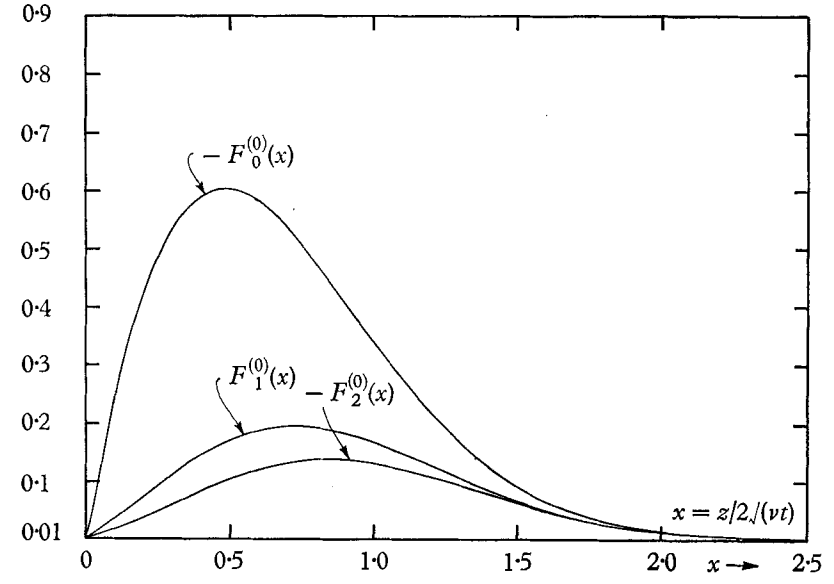

Non-dimensional distance normal to the plate

FIGURE 2. Plot of $F_n^{(0)}(x)$, $n = 0, 1, 2$.

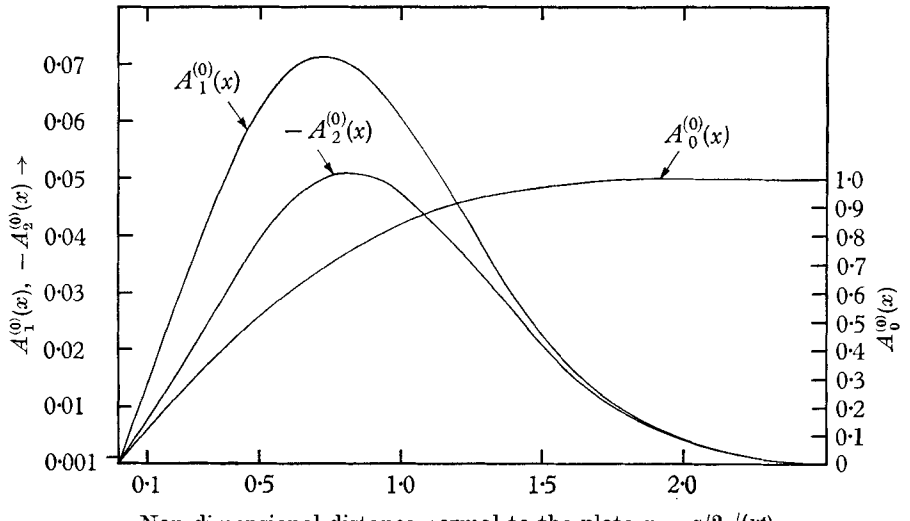

Non-dimensional distance normal to the plate $x = z/2\sqrt{(\nu t)}$

FIGURE 3. Plot of $A_n^{(0)}(x)$, $n = 0, 1, 2$.

convective accelerations. If, *a priori*, we infer that $\phi \sim O(1)$ and $\phi_\xi \sim O(1/\xi)$, the convective accelerations –4– and –*c*– are an order ξ^{-4} smaller than, say, the local acceleration or any of the remaining terms. Define B, a kind of Rossby number, as the ratio of the radial convective acceleration to the centrifugal acceleration. From the above considerations, in the plate boundary layer,

$$B = \xi^{-4},$$

and –4– and –*c*– act as perturbations on the over-all momentum balance. For large values of ξ we equate the right-hand sides of (18) and (19) to zero and a similarity solution of (18) implies that the angular momentum must equal $\operatorname{erf}(\frac{1}{2}\zeta)$. The convective accelerations, when taken into account, will introduce correction terms of the order B^n, where $n = 1, 2, 3, \ldots$. We can then formalize the procedure and write

$$\phi^{(0)}(\xi, \zeta) = \sum_{n=0}^{N-1} \xi^{-4n} \phi_n^{(0)}(x), \quad x = \tfrac{1}{2}\zeta, \tag{21}$$

and

$$A^{(0)}(\xi, \zeta) = \sum_{n=0}^{M-1} \xi^{-4n} A_n^{(0)}(x), \tag{22}$$

where $\phi_n^{(0)}(\zeta)$ and $A_n^{(0)}(\zeta)$ are unknown functions of ζ, and N and M are the number of terms retained in these series. Substitute (21) and (22) into (17) and (18) and equate the coefficients of ξ^{-4n} to zero. Using quadratures we then solve for the first few of the x-dependent coefficients found in expressions (21) and (22). Figures 2 and 3 show these coefficients plotted versus $x = \frac{1}{2}\zeta$.

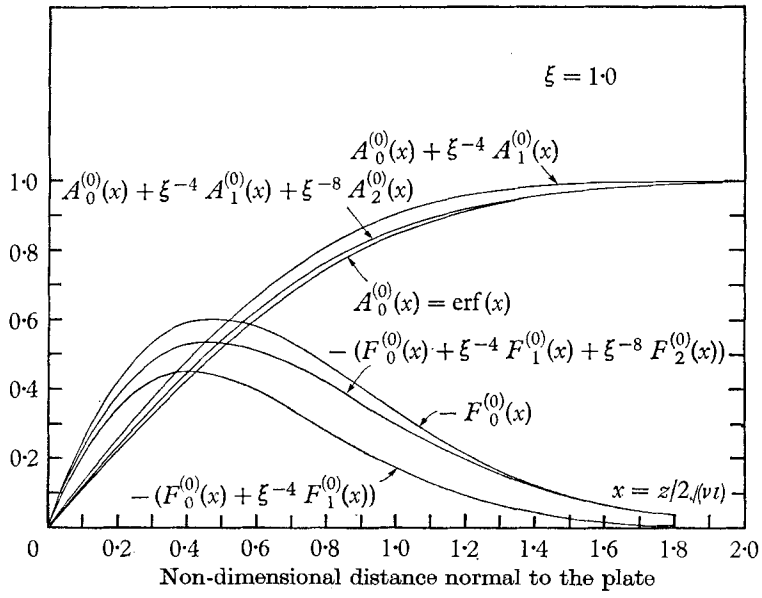

FIGURE 4. Plot of $2\xi^3 u$ and ξv, at $\xi = 1{\cdot}0$, when one, two or three terms are retained in the asymptotic expansions of these functions.

The plate boundary-layer functions can then be written as

$$\left.\begin{aligned} u(\xi,\eta;\epsilon) &= \frac{1}{2\xi^3}\left(F_0^{(0)}(x)+\frac{F_1^{(0)}(x)}{\xi^4}+\frac{F_2^{(0)}(x)}{\xi^8}+\ldots\right)+O(\sqrt{\epsilon}),\\ v(\xi,\eta;\epsilon) &= \frac{1}{\xi}\left(\operatorname{erf}(x)+\frac{A_1^{(0)}(x)}{\xi^4}+\frac{A_2^{(0)}(x)}{\xi^8}+\ldots\right)+O(\sqrt{\epsilon}),\\ w(\xi,\eta;\epsilon) &= \frac{\sqrt{\epsilon}}{\xi^4}\left(2\phi_0^{(0)}(x)+\frac{6}{\xi^4}\phi_1^{(0)}(x)+\frac{10}{\xi^8}\phi_2^{(0)}(x)+\ldots\right)+O(\epsilon),\\ \text{and}\qquad \Psi(\xi,\eta;\epsilon) &= \frac{\sqrt{\epsilon}}{\xi^2}\left(\phi_0^{(0)}(x)+\frac{\phi_1^{(0)}(x)}{\xi^4}+\frac{\phi_2^{(0)}(x)}{\xi^8}+\ldots\right)+O(\epsilon), \end{aligned}\right\} \tag{23}$$

where $x = \frac{1}{2}\zeta = z/2\sqrt{(\nu t)}$. It can be shown (Barcilon 1965*a*) that $F_0^{(0)}(x)$ and $\phi_0^{(0)}(x)$ are negative functions of x while $A_1^{(0)}$ is a positive function of x for $0 < x < \infty$. Figure 4 shows the functions $2\xi^3 u$ and $A = \xi v$ when one, two, and three terms are retained and when $\xi = 1{\cdot}0$.

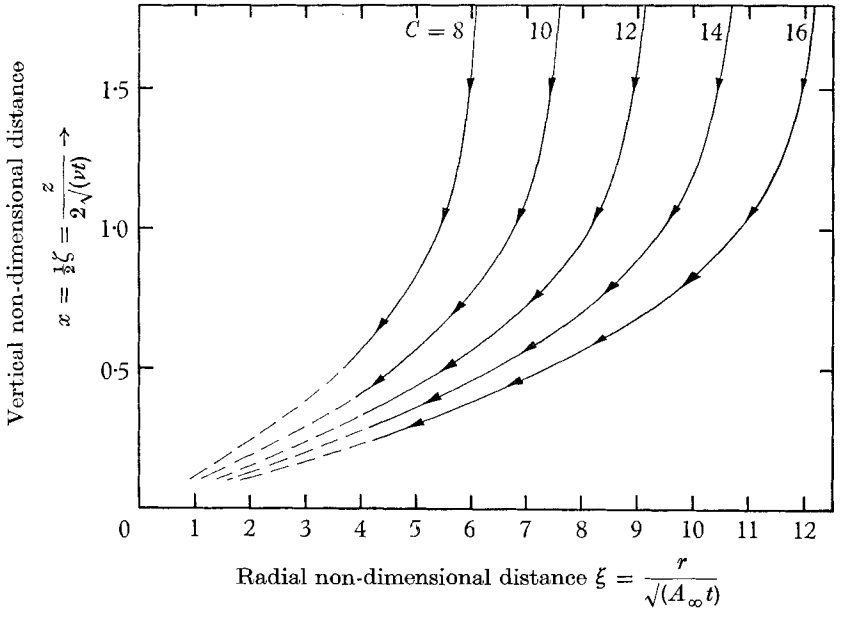

FIGURE 5. Projection of the streamline in the (ξ, x)-plane.

We shall conjecture that the error made in truncating these series is of the order of the first neglected term. Then, by keeping in turn one or two terms and by requiring an accuracy of 10^{-2} or 10^{-3} we find that these series verify such an accuracy criterion for values of $\xi > \xi_0$ where ξ_0 is a constant ranging from 1·2 to 3·4.

We retain the first term in the series listed in (25) and look at the projection of the streamlines in the (ξ, x)-plane. These curves satisfy an equation of the form

$$\xi = C\sqrt{(|\phi_0^{(0)}(x)|)},$$

where C is a constant of integration. The resulting curves are shown in figure 5. Fluid from the inviscid region sinks into the plate boundary layer and as it approaches the plate it acquires a radial inward motion.

4. Order $\sqrt{\epsilon}$ inviscid solution

In the plate boundary layer, the fluid that is forced toward the axis erupts near the origin and proceeds in an axial direction. Since there is no sink along the axis at infinity, this slug of fluid pushes on to the surrounding fluid, and we might anticipate that the axial boundary layer will affect the inviscid region like a line source. The inviscid-region flow then links the axial boundary-layer flow to the plate boundary flow. The potential vortex flow, which represents the leading term in the ϵ-expansion of the inviscid flow, is purely azimuthal: the meridional motion in the inviscid region is then described by the $O(\sqrt{\epsilon})$ terms.

Let us outline the inviscid solution and its pitfalls. For a more detailed treatment the reader is referred elsewhere (Barcilon 1965*a* or *b*). The $O(\sqrt{\epsilon})$ inviscid flow is coupled to the $O(\epsilon^0)$ plate boundary-layer flow through the prescription of the vertical velocity at the edge of the plate boundary layer. Because we only know the vertical velocity at the edge of the plate boundary for $R > \xi_0$, we have to restrict our investigation of the inviscid region to the domain

$$\xi_0 \leqslant R \leqslant \infty, \quad 0 < \theta < \tfrac{1}{2}\pi.$$

On the arc $0 < \theta < \frac{1}{2}\pi$, $R = \infty$, we demand that the entire flow be identical to the potential vortex flow, and the boundary condition in the vicinity of the axis and on the arc $0 < \theta < \frac{1}{2}\pi$, $R = \xi_0$ are unknown at this stage. Substitute the $O(\sqrt{\epsilon})$ terms of the inviscid ϵ expansions of the dependent functions into the governing equations and collect terms of order $\sqrt{\epsilon}$. By considering the angular-momentum equation so obtained, we find that the angular momentum of $O(\sqrt{\epsilon})$ remains constant on rays $\theta =$ const. The boundary conditions on the arc $R = \infty, 0 < \theta < \frac{1}{2}\pi$ require that this constant be identically zero. As a result, the meridional and azimuthal motions are uncoupled: a fluid particle, by conserving its angular momentum, does not offer any resistance to lateral displacements.

Let the inviscid ϵ expansion for the pressure be written as

$$p(R, \theta; \epsilon) = -\tfrac{1}{2}R^2 \sin^2\theta + \epsilon^{\frac{1}{2}} p^{(1)}(R, \theta) + \ldots,$$

where the leading term represents the free vortex pressure. The $O(\sqrt{\epsilon})$ meridional inviscid motion is then described in terms of a single equation

$$\nabla^2 p^{(1)} = 0, \tag{24}$$

where ∇^2 is the spherical Laplacian operator with the azimuthal dependence deleted. Let us point out that this equation holds for the entire inviscid region since we only made use of the boundary conditions at infinity and assumed a potential vortex to prevail as the $O(\epsilon^0)$ flow in that region. However, due to the restricted knowledge of the boundary conditions we shall arrive at an incomplete solution of the flow in a domain bounded by $R > \xi_0$, $0 < \theta < \frac{1}{2}\pi$. In that domain, the solution of (24) in separable form is a standard one; namely we can express $p^{(1)}(R, \theta)$ as

$$p^{(1)}(R, \theta) = \sum_{\ell} R^{-\ell-1}[C_\ell P_\ell(\mu) + D_\ell Q_\ell(\mu)], \tag{25}$$

where $\mu = \cos\theta$ and where P_ℓ and Q_ℓ are the Legendre functions of the first and second kind. The geometry does not demand integer values for the separation constant ℓ, nevertheless we shall assume, from here on, that ℓ is a positive integer.

The boundary condition at $R = \infty$ is automatically satisfied by the form represented in (25). The boundary condition on the plate, namely on $R > \xi_0$, $\theta = \frac{1}{2}\pi$, leads to a set of equations in which the Legendre functions evaluated at $\mu = 1$ are the coefficients of the C_ℓ and D_ℓ. Due to the parity character of these functions, only the C_{2j+1} and D_{2j} are determined by the use of the plate boundary condition. The $Q_\ell(\mu)$ being singular at $\mu = 1$, the flow behaviour in the vicinity of the axis is controlled by these singular functions: by matching the inviscid solution to the axial boundary-layer solution we shall only be able to determine the D_{2j+1} coefficients. The remaining set of unknown coefficients, namely the C_{2j}, are determined if we assume that the pressure $p^{(1)}(R, \theta)$ is given on the arc $R = \xi_0$, $0 < \theta < \frac{1}{2}\pi$, say $p^{(1)}(R, \theta) = \pi_0(\mu)$. After some manipulations we find that the C_{2j} not only depend on $\pi_0(\mu)$, but they are also expressed in terms of the D_{2j+1} and the D_{4j+2} coefficients which are determined respectively by the axial and plate boundary conditions.

All these coefficients are a measure of the sink or source strengths of the axial and plate boundary layers and their interdependence shows that the flow in various regions is intimately linked to all the others.

To complete the problem we require a solution of the axial boundary-layer flow. In this region we must retain a balance in the radial direction between the centrifugal acceleration and the radial pressure gradient. As a result the boundary-layer differential equations for the axial region are four in number. Furthermore, the plate boundary layer, as will be seen shortly, erupts near the origin and discharges mass into the axial boundary layer. Thus we must know more about this mechanism before being able to tackle the axial flow. Nevertheless, from the inviscid solution we can deduce that, for large R, the ratio w/u tends to zero as $\theta \log \theta$ when θ tends to zero.

5. Plate boundary-layer solution for small ξ

To understand the eruption of the plate boundary-layer flow into the axial boundary layer we must first find a solution of the plate boundary-layer flow for values of ξ of $O(1)$. The solution of § 3 was based on the fact that, for $\xi > \xi_0$, vorticity is primarily redistributed by a diffusive mechanism; i.e. the Rossby number was small. The radial velocity of a fluid particle found in the plate boundary layer increases as this particle approaches the axis. Thus, we anticipate that for $O(D(\epsilon)) < \xi < \xi_0$ the convective accelerations will be of the same order of magnitude as the centrifugal acceleration; i.e. the previously defined Rossby number B becomes of order unity in this region. (Here $D(\epsilon)$ is the radius of the axial core at its base.) As a result, we must retain the non-linear terms in the plate boundary-layer equations and these equations are solved by using approximate methods.

Let $\epsilon^{\frac{1}{2}}\Delta(\xi)$ be the thickness of the plate boundary layer at point ξ and define τ as

$$\tau = \eta/\epsilon^{\frac{1}{2}}\Delta(\xi),$$

so that τ equals zero at the plate and unity at the edge of the plate boundary

layer. The η-averaged radial and circumferential plate boundary-layer equations read

$$-2\alpha\xi^2\frac{d}{d\xi}\left[\frac{q(\xi)}{\xi}\right]+\beta\frac{d}{d\xi}\left[\frac{q^2(\xi)}{\xi\delta(\xi)}\right]+16\gamma\left[\frac{\delta(\xi)}{\xi^2}\right]+\frac{f'_{(0)}}{4}\left[\frac{q(\xi)}{\delta(\xi)}\right]=0, \tag{26}$$

and

$$2b\xi^3\frac{d}{d\xi}\left[\frac{\delta(\xi)}{\xi}\right]+\lambda\left(\frac{dq}{d\xi}\right)+\frac{k'_{(0)}}{4}\left[\frac{\xi}{\delta(\xi)}\right]=0, \quad ' \equiv \frac{d}{d\tau}. \tag{27}$$

In the above equations α, β, γ, λ, b and a are defined as

$$\alpha=\int_0^1 f(\tau)\,d\tau, \quad \beta=\int_0^1 f^2(\tau)\,d\tau,$$

$$\gamma=\int_0^1 (1-k^2(\tau))\,d\tau, \quad \lambda=\int_0^1 f(\tau)\,[k(\tau)-k(1)]\,d\tau,$$

and

$$b=k(1)-a, \quad a=\int_0^1 k(\tau)\,d\tau,$$

where we have assumed that u and v can be written as

$$u=\{\Omega(\xi)/\xi\}f(\tau), \tag{28}$$

and

$$v=(1/\xi)\,k(\tau). \tag{29}$$

$f(\tau)$ and $k(\tau)$ will be called the shape functions since, at a given ξ, they determine the shape of the velocity profiles. The two unknown dependent functions are $\delta(\xi)$ and $q(\xi)$. $\delta(\xi)$ is the normalized plate boundary-layer thickness defined as

$$\delta(\xi)=\Delta(\xi)/\Delta(\infty)=\Delta(\xi)/4{\cdot}0;$$

$\epsilon^{\frac{1}{2}}\Delta(\infty)$ is the constant thickness of the plate boundary layer for large values of ξ. The value of $\Delta(\infty)$ was taken as follows: for large ξ, when x equals 2·0, i.e. when η equals $4\epsilon^{\frac{1}{2}}$, $F_0^{(0)}(2)$ and $\mathrm{erf}(2)$ equal respectively $-0{\cdot}012$ and 0·995. Both functions are then within 1 % of their value in the inviscid flow where $F_0^{(0)}(\infty)=0$ and $\mathrm{erf}(\infty)=1{\cdot}0$. We then define the plate boundary-layer thickness as the distance we have to move away from the plate for the velocity profiles to be within 1 % of their inviscid value. Finally, the other dependent function $q(\xi)$ is defined as

$$q(\xi)=Q(\xi)/2\pi\alpha, \tag{30}$$

where $\epsilon^{\frac{1}{2}}Q(\xi)$ measures the flux across the plate boundary layer at point ξ and equals $2\pi\int_0^{\epsilon^{\frac{1}{2}}\Delta(\xi)}\xi u(\eta)\,d\eta$.

As boundary conditions we demand that for large ξ

$$\delta(\xi)=1 \tag{31}$$

and

$$q(\xi)=\phi_0^{(0)}(\infty)/\alpha\xi^2, \quad \phi_0^{(0)}(\infty)=-0{\cdot}585. \tag{32}$$

This last condition can easily be obtained if we substitute the leading term of the asymptotic expansion of u in the expression for $Q(\xi)$ and the resulting expression in (30).

Equations (26), (27), (31), and (32) constitute our basic differential system. To solve such a system the shape functions $f(\tau)$ and $k(\tau)$ must be specified. These

functions must satisfy the boundary conditions at the plate and at the edge of the boundary layer and must be such that the expressions for u and v, namely (28) and (29), agree for large values of ξ with the leading terms of the corresponding quantities found in (23). If we let

$$f(\tau) = \tfrac{1}{2}F_0^{(0)}(C\tau) \tag{33}$$

and

$$k(\tau) = \operatorname{erf}(C\tau), \tag{34}$$

where C is an undetermined constant, we must demand that as $\xi \to \infty$, $C\tau$ tends to $\eta/2\sqrt{\epsilon}$, or after making use of the definition of τ we find that C must equal $\Delta(\infty)/2{\cdot}0 = 2{\cdot}0$.

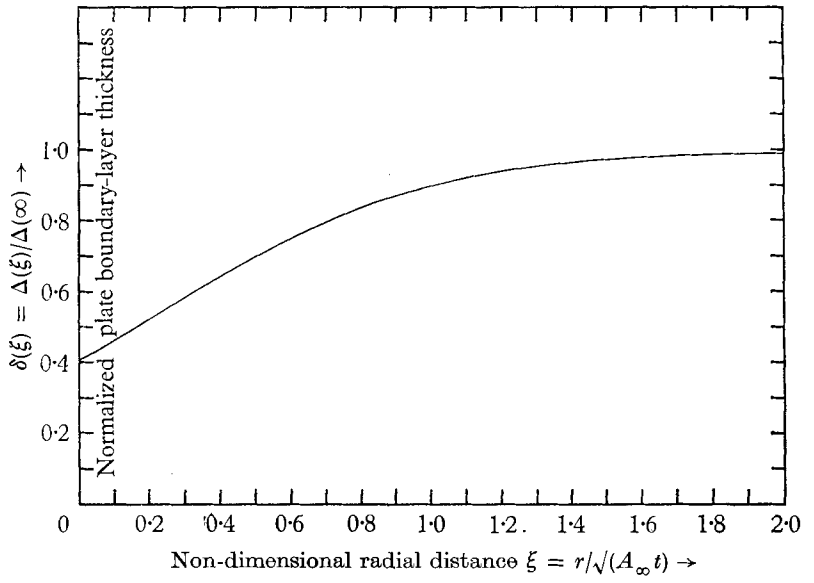

FIGURE 6. Plot of the normalized plate boundary-layer thickness *vs.* ξ.

The differential system (26), (27), (31) and (32) was solved numerically on an IBM 7094: the integration was started at $\xi = 4{\cdot}1$ and was continued until $\xi = 0$. Figure 6 shows the variation of $\delta(\xi)$ with ξ: the normalized plate boundary-layer thickness is a slowly increasing function of ξ that reaches its asymptotic value when ξ is in the vicinity of 2·0. Figure 7 illustrates the variations with ξ of the plate boundary-layer flux $Q(\xi)$ and of the function $\Omega(\xi)$. See (28) for the definition of $\Omega(\xi)$. $Q(\xi)$ is a negative function of ξ that has its maximum at $\xi = 0$. This means that the fluid, trapped in the plate boundary layer, moves inward in this layer until it gets very close to the origin, before it erupts and moves upward along the axis. Finally, the equation of the projection of a given streamline in a plane parallel to the plate is given by

$$\int_0^{\psi} d\psi = \frac{\operatorname{erf}(\tau)}{F_0^{(0)}(2\tau)} \int_{4{\cdot}1}^{0} \frac{d\xi}{\xi\,\Omega(\xi)}, \tag{35}$$

where ψ is the azimuthal angle. In (35) as $\tau \to 1$, $\operatorname{erf}(2\tau)/F_0^{(0)}(2\tau)$ becomes a large number, i.e. the orbit of a given particle is nearly circular at the edge of the

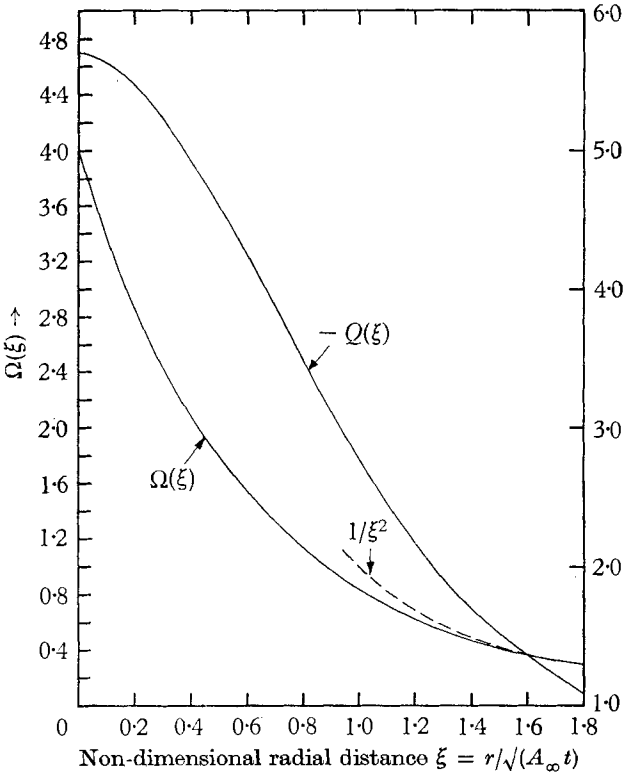

FIGURE 7. Plot of the plate boundary-layer mass flux $Q(\xi)$ and of $\Omega(\xi)$ *vs.* ξ.

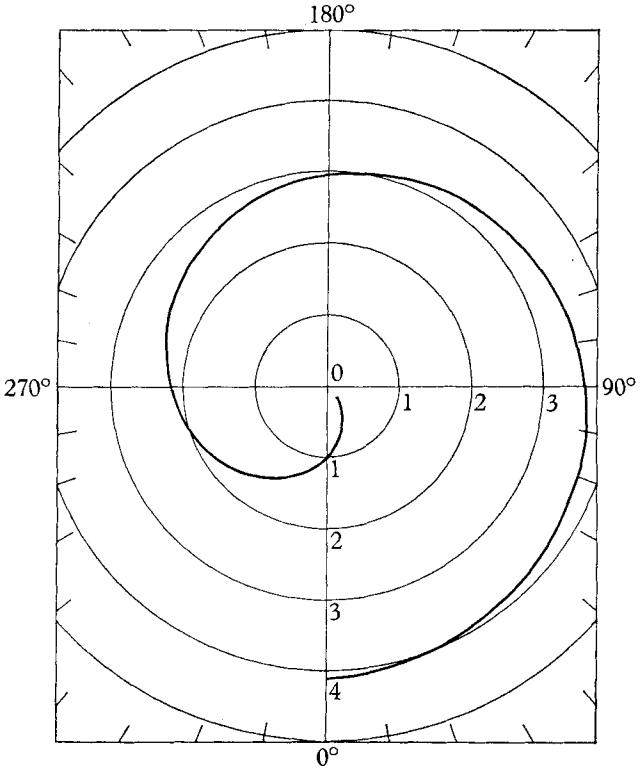

FIGURE 8. Plot of a given streamline in the vicinity of the plate.

boundary layer. Figure 8 shows a given streamline in the immediate vicinity of the plate: a fluid particle near the plate approaches the origin in a spiral-like trajectory.

6. Flow behaviour near the origin

When ξ is in the vicinity of the origin and for moderate values of τ, from (33) and (34) we can estimate the radial and the circumferential velocities to be $O(1/\xi)$. If we write the radial plate boundary-layer momentum equation as

$$\underbrace{-\frac{1}{2}\left[\frac{\partial}{\partial\xi}(\xi u)+\zeta\frac{\partial u}{\partial\zeta}\right]}_{\text{-1-}}+\underbrace{\left(u\frac{\partial u}{\partial\xi}+w\frac{\partial u}{\partial\zeta}\right)}_{\text{-2-}}+\underbrace{\xi^{-3}(1-A^2)}_{\text{-3-}}=\underbrace{\frac{\partial^2 u}{\partial\zeta^2}}_{\text{-4-}}, \tag{36}$$

where

$$\zeta=\eta/\sqrt{\epsilon},$$

we can readily estimate –1–, –2–, –3– and –4– to be:

$$\left.\begin{aligned}&\text{-1-}\sim\text{-4-}\sim O(\xi^{-1}),\\&\text{-2-}\sim\text{-3-}\sim O(\xi^{-3}).\end{aligned}\right\} \tag{37}$$

In the above equation –1– represents the local radial acceleration, –2– is the convective radial acceleration, while –3– represents the difference between the radial pressure gradient and the centrifugal acceleration. Finally, –4– denotes the radial viscous forces. From the order of magnitude listed in (37) we deduce that the flow near the origin can be considered as *steady* and *inviscid* since –1– and –4– are an order ξ^2 smaller than –2– and –3–. Consider a ring of plate boundary-layer fluid bounded by radii ξ and $\xi+d\xi$ and having a height $\epsilon^{\frac{1}{2}}\Delta(\xi)$. As this ring contracts to zero, the area of the rigid boundary in contact with that fluid diminishes: viscous forces are insufficient to slow down the inrushing fluid. This fluid is slowed down and forced upward by the pressure that builds up at the origin. As a result, the turning is controlled by an inviscid mechanism. To be sure, viscous boundary layers are still needed on the plate and along the axis, but these layers are deeply embedded in the corner region flow.

Near the origin, the governing equations are then:

$$\left.\begin{aligned}&u\frac{\partial u}{\partial\xi}+w\frac{\partial u}{\partial\zeta}+\frac{\partial p}{\partial\xi}-\frac{v^2}{\xi}=0,\\&u\frac{\partial A}{\partial\xi}+w\frac{\partial A}{\partial\zeta}=0,\\&u\frac{\partial w}{\partial\xi}+w\frac{\partial w}{\partial\zeta}+\frac{\partial p}{\partial\zeta}=0,\\&\frac{\partial}{\partial\xi}(\xi u)+\frac{\partial}{\partial\zeta}(\xi w)=0.\end{aligned}\right\} \tag{38}$$

Let us consider a given streamline that links the plate boundary layer to the axial boundary layer. Let us label as station A the first point on that streamline that lies in the plate boundary-layer region, and as B the first point on that same streamline that lies in the axial boundary-layer region. By knowing the conditions

at station A, we shall be able to infer some of the flow characteristics of station B. On that streamline we shall write Bernoulli's equation, the conservation of mass and of angular momentum. At station B, we shall approximate the radial momentum equation by

$$\frac{\partial p}{\partial \xi} - \frac{v^2}{\xi} = 0. \tag{39}$$

Define the stretched variables y and ρ as

$$y = \eta/\epsilon^{\frac{1}{2}}\Delta(0)$$

and

$$\rho = \xi/D(\epsilon),$$

where $\epsilon^{\frac{1}{2}}\Delta(0)$ is the plate boundary-layer thickness near the origin and where $D(\epsilon)$ is the thickness of the base of the axial core. $D(\epsilon)$ is an unknown function of ϵ.

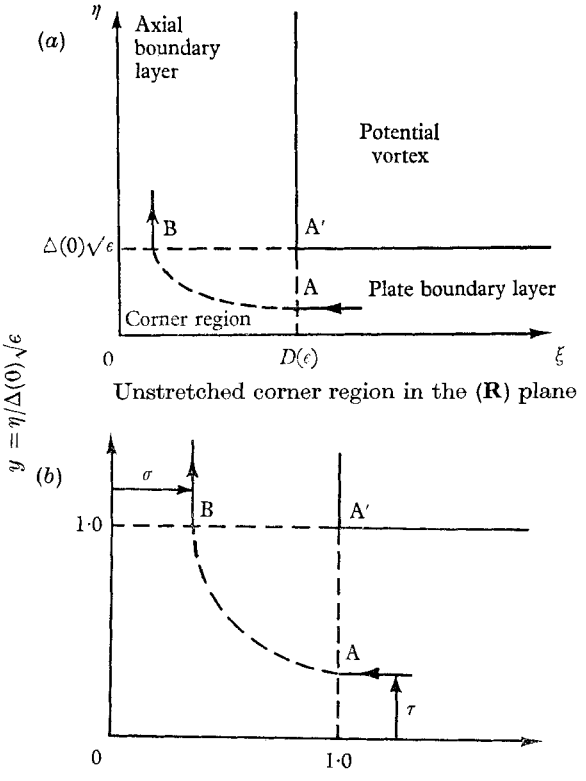

FIGURE 9. (*a*) Unstretched corner region in the (**R**)-plane.
(*b*) Stretched corner region in the (**R**)-plane.

Define σ and τ so that in the stretched diagram of the corner region A and B are located respectively at $(1, \tau)$ and $(\sigma, 1)$. Here σ is an unknown function of τ. The reader is referred to figure 9, where all the above functions are graphed.

Let subscripts A and B signify flow quantities at stations A and B. Conservation of angular momentum implies that $v_A(\tau)$ and $v_B(\sigma)$ relate through the relation

$$v_A(\tau) = \sigma v_B(\sigma). \tag{40}$$

Conservation of mass requires that

$$2\pi\epsilon^{\frac{1}{2}}\Delta(0)\,D(\epsilon)\int_0^{\tau} u_{\mathrm{A}}(y)\,dy + 2\pi D^2(\epsilon)\int_0^{\sigma} w_{\mathrm{B}}(\rho)\,\rho\,d\rho = 0,$$

or, after a differentiation with respect to τ, the above equation simplifies to

$$-2\lambda u_{\mathrm{A}}(\tau) = w_{\mathrm{B}}(\beta)\,d\beta/d\tau, \tag{41}$$

where the parameter λ is defined as

$$\lambda = \epsilon^{\frac{1}{2}}\Delta(0)/D(\epsilon),$$

and where $\beta(\tau)$, the normalized cross-sectional area of the core, is defined as

$$\beta(\tau) = \sigma^2(\tau).$$

Both $\beta(\tau)$ and $\lambda(\epsilon)$ are unknown functions at this stage. Bernoulli's equation, written for the streamline AB, relates quantities at stations A and B by the following relation:

$$p_{\mathrm{A}} + \tfrac{1}{2}[u_{\mathrm{A}}^2(\tau) + v_{\mathrm{A}}^2(\tau) + w_{\mathrm{A}}^2(\tau)] = p_{\mathrm{B}} + \tfrac{1}{2}[u_{\mathrm{B}}^2(\beta) + v_{\mathrm{B}}^2(\beta) + w_{\mathrm{B}}^2(\beta)].$$

Since w_{A}^2 is an order ϵ smaller than $(u_{\mathrm{A}}^2 + v_{\mathrm{A}}^2)$ and since we anticipate u_{B}^2 to be much smaller than $(v_{\mathrm{B}}^2 + w_{\mathrm{B}}^2)$, we can approximate the above equation by

$$p_{\mathrm{A}} + \tfrac{1}{2}[u_{\mathrm{A}}^2(\tau) + v_{\mathrm{A}}^2(\tau)] = p_{\mathrm{B}} + \tfrac{1}{2}[v_{\mathrm{B}}^2(\beta) + w_{\mathrm{B}}^2(\beta)]. \tag{42}$$

The plate boundary layer being thin, the pressure at A′ (see figure 9) equals the pressure at A, i.e.

$$p_{\mathrm{B}} - p_{\mathrm{A}} = p_{\mathrm{B}} - p_{\mathrm{A}'} = \int_1^{\sigma} v_{\mathrm{B}}^2(\rho)\frac{d\rho}{\rho}, \tag{43}$$

where the above equation represents the line integral of (39) along A′A. (40), (41), (42) and (43) constitute our basic equations and β, $v_{\mathrm{B}}(\beta)$, $w_{\mathrm{B}}(\beta)$ and $(p_{\mathrm{B}} - p_{\mathrm{A}})$ are our unknowns. We can eliminate† $v_{\mathrm{B}}(\beta)$, $w_{\mathrm{B}}(\beta)$ and $(p_{\mathrm{B}} - p_{\mathrm{A}})$ between these basic equations; the problem reduces to the determination of $\beta(\tau)$; namely we have to solve

$$\frac{d\beta}{d\tau} = \frac{2\lambda\,|F_0^{(0)}(2\tau)|}{\left\{F_0^{(0)^2}(2\tau) + \frac{2}{\pi}\int_{\tau}^{1} \operatorname{erf}(2x)\exp(-4x^2)\,[\beta^{-1}(x) - 1]\,dx\right\}^{\frac{1}{2}}} \tag{44}$$

with

$$\beta(0) = 0, \quad \beta(1) = 1. \tag{45}$$

The above differential system is a two-point boundary-value problem for the function $\beta(\tau)$ and the parameter λ plays a role similar to that played by an eigenvalue in linear boundary-value problems: the condition on β at $\tau = 0$ will only be satisfied for a given value of λ. By starting at $\tau = 1$, we integrated numerically the above differential system on an IBM 7094. For an accuracy of 10^{-3}, the integration yielded the following value for λ:

$$\lambda = 0{\cdot}689,$$

and therefore $D(\epsilon)$ reads

$$D(\epsilon) = \epsilon^{\frac{1}{2}}\Delta(0)/\lambda = 2{\cdot}487\epsilon^{\frac{1}{2}} \approx 2{\cdot}5\epsilon^{\frac{1}{2}}.$$

† Barcilon (1965*b*).

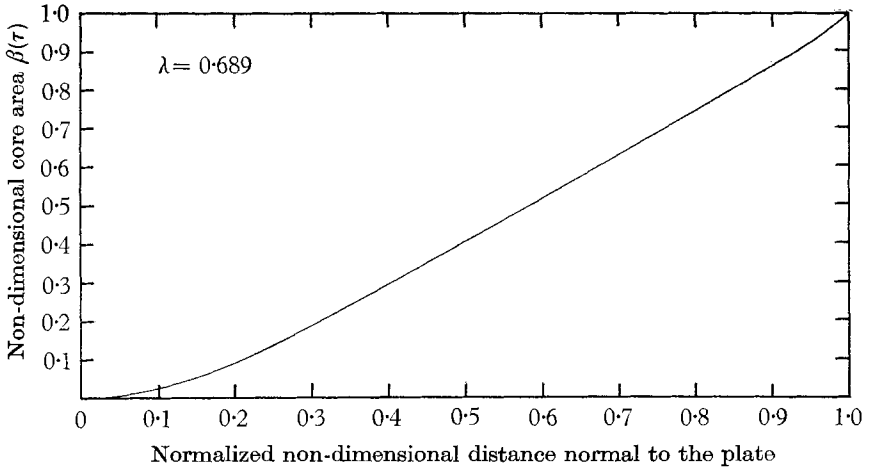

FIGURE 10. Plot of $\beta(\tau)$ *vs.* τ.

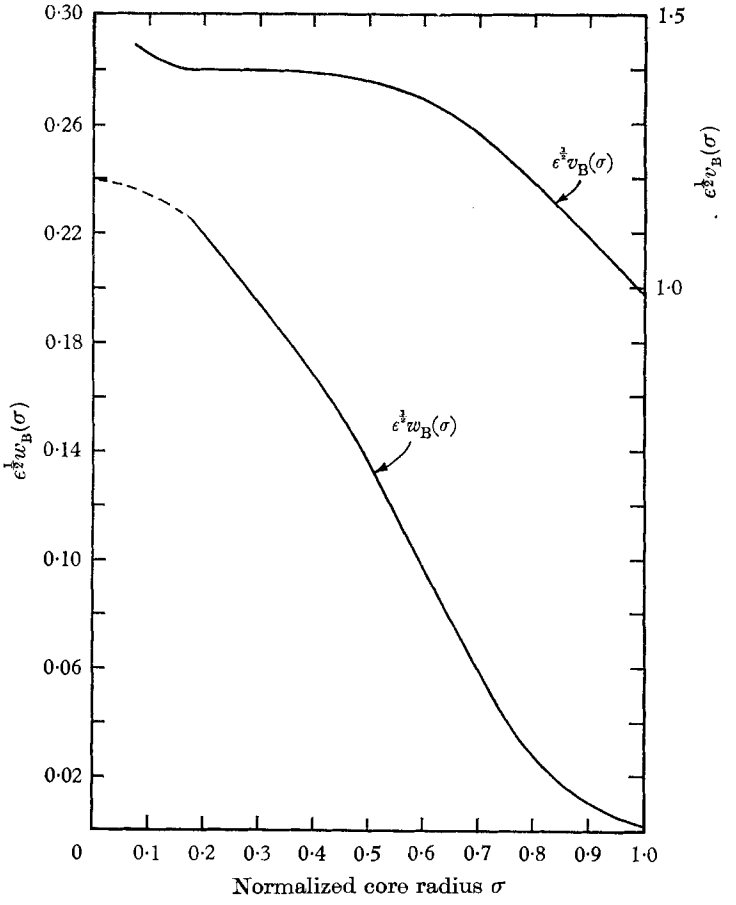

FIGURE 11. Plot of $\epsilon^{\frac{1}{2}}w_B(\sigma)$ and $\epsilon^{\frac{1}{2}}v_B(\sigma)$ *vs.* σ.

The diameter of the base of the axial core has the same order of magnitude as the thickness of the plate boundary layer. Figure 10 shows the variations of $\beta(\tau)$ *vs.* τ for the above value of λ. In the range $0{\cdot}15 \leqslant \tau \leqslant 1{\cdot}0$, β is approximately a linear function of τ with a slope $a = 1{\cdot}156$, while for $0 \leqslant \tau \leqslant 0{\cdot}15\,\beta$ approaches the origin with zero slope. Care must be exercised when using the function $\beta(\tau)$. The assumption that the fluid is inviscid invalidates such a function in the vicinity of $\tau = 0$. Nevertheless, using $\beta(\tau)$ away from the value $\tau = 0$ we obtain, at station B, an approximate representation of the variations of the velocity profiles with radius. The vertical and circumferential velocities at B are

$$w_{\mathrm{B}}(\beta) = -\lambda \frac{F_0^{(0)}(2\tau)}{D(\epsilon)\,(d\beta/d\tau)},$$

and

$$v_{\mathrm{B}}(\beta) = \frac{\operatorname{erf}(2\tau)}{D(\epsilon)\,\beta(\tau)}.$$

In the region where $\beta(\tau)$ is approximately linear, $(d\beta/d\tau)$ is nearly constant; i.e. the vertical velocity at B, when expressed as a function of τ, is proportional to the radial velocity at A and has a magnitude of $O(D^{-1}(\epsilon)) \sim O(\epsilon^{-\frac{1}{2}})$. At B, $v_{\mathrm{B}}(\beta)$ is also $O(1/\epsilon^{\frac{1}{2}})$. Figure 11 shows the variations of $v_{\mathrm{B}}(\sigma)$ *vs.* $\sigma = \beta^{\frac{1}{2}}$.

7. Experimental flows

It is desirable to verify, qualitatively, some of the results of the previous theoretical investigation using some experimental observations. In particular, we want to test the hypothesis that the plate boundary-layer flow erupts in the immediate vicinity of the origin and we want to verify that the diameter of the base of the axial core is of the same order of magnitude as the plate boundary-layer thickness. We are then especially interested in modelling the flow behaviour in the vicinity of the axis and of the plate. An experiment modelling the decay of a vortex normal to a stationary disc presents a number of problems, owing to the unsteady character of the flow. In the (**R**)-plane, the 'steady' flow in the vicinity of the origin is governed by the same set of equations and boundary conditions as the steady corner flow obtained when a vortex swirls on top of a stationary disk. If p' denotes the departure from the hydrostatic pressure we have a correspondence between

$$(\xi, \eta, u, v, w, A, p, \epsilon) \quad \text{and} \quad (r^*, z^*, u^*, v^*, w^*, A^*, p^*, \epsilon^*).$$

The non-dimensional * quantities relate to the dimensional ′ quantities through the relations

$$r^* = r/L, \quad z^* = z/L,$$
$$u^* = u'L/A_0, \quad v^* = v'L/A_0,$$
$$w^* = w'L/A_0, \quad A^* = A'/A_0,$$
$$p^* = (p'/\rho')\,(L/A_0)^2, \quad \epsilon^* = \nu/A_0;$$

ν is the constant kinematic viscosity, A_0 is the prevailing angular momentum in the steady vortex flow and L is a characteristic length.

For our experimental flow, the apparatus consisted of a glass cylinder of radius $L = 10\,\mathrm{cm}$ glued on top of a flat glass plate. Water, with $\nu = 0{\cdot}01\,\mathrm{cm}^2/\mathrm{sec}$ at

room temperature, was injected tangentially in the cylinder by means of an array of nozzles and was removed along the axis by means of a coaxial tube. When the prevailing angular momentum A_0 was of the order of 40 cm^2/sec, the free surface depression was small compared with the height of the water in the container. We assumed the free-surface effects and the side-walls effects to be small near the centre of the disk. The observations of the plate boundary-layer flow and of the corner region flow showed that: the flow was laminar except in the immediate vicinity of the origin; fluid moved, in the plate boundary layer, along spiral-like streamlines and erupted in the immediate vicinity of the axis. By observing the curvature of the streaklines emitted from a large crystal (a few mm) of potassium permanganate sitting on the bottom plate, we could estimate the plate boundary-layer thickness to range from 2 to 4 mm while the radius of the filament that erupted at the axis was estimated to be of the order of 1 to 2 mm. The prevailing angular momentum A_0 was measured by timing the fluid particle located at a given distance from the axis of rotation. For $A_0 = 40$ cm^2/sec and $\nu = 0{\cdot}01$ cm^2/sec, the experimental dimensionless number ϵ^* equals $2{\cdot}5 \times 10^{-4}$; when L is taken as 10 cm, $\epsilon^{*\frac{1}{2}}L$ equals 1·6 mm. Therefore the plate boundary-layer thickness and the core thickness at the eruption agree with the predicted results.

8. Vortex breakdown: theoretical model

In the experimental flow, the plate boundary-layer fluid erupts into a thin filament 1–2 mm in diameter which bursts into a much wider core having a diameter between 3 and 4 cm. Such a phenomenon is called a vortex breakdown and seems to have been first noticed a few years ago by people working on the aerodynamics of delta wings. The reader is referred to Benjamin (1962) for a complete bibliography on this subject. The vortex breakdown phenomenon is still not very well understood, and various hypotheses have been proposed for its explanation. Benjamin (1962) ruled out the hypothesis that the vortex breakdown was an instability phenomenon and pointed out the analogy with the hydraulic jump found in channel flows. In what follows we shall adopt the latter point of view and offer a simple theoretical model explaining this phenomenon.

Consider an axial, steady, inviscid, cylindrical jet forced along the axis of a potential vortex flow in an unbounded fluid. Assume that the vertical velocity in the jet is uniform across its cross-section and that at any such cross-section the pressure is a constant dictated by the value of the vortex pressure at the outer edge of the jet and at that same level. Let D_1, W_1 be the radius of the jet and its vertical velocity before the breakdown, while D_2 and W_2 denote the corresponding quantities after the breakdown. These quantities are shown in figure 12. Conservation of mass implies

$$D_1^2 W_1 = D_2^2 W_2, \tag{46}$$

on the cross-section $a_1 b_1$ the pressure force is

$$-\rho\left(\frac{A_0^2}{2D_1^2}\right)(\pi D_1^2) = -\rho A_0^2 \pi/2,$$

where ρ is the constant fluid density and A_0 the prevailing angular momentum.

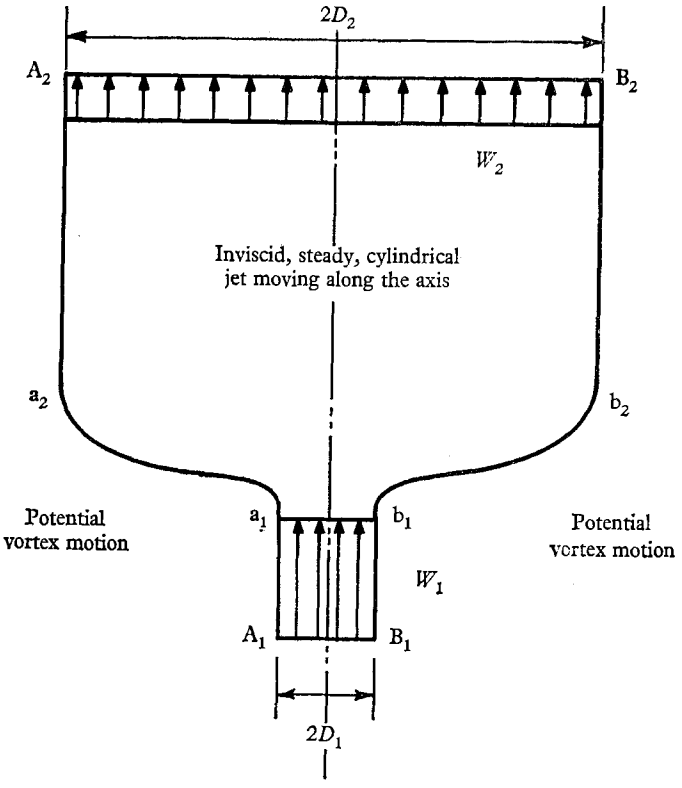

FIGURE 12. Free-body diagram illustrating the vortex break-down phenomenon.

Similarly, on the cross-section $a_2 b_2$ the pressure force is $-\rho A_0^2 \pi/2$; i.e. these two pressure forces cancel. The only pressure force in the vertical results from the pressure exerted on the side $a_1 a_2$ and $b_1 b_2$. The net upward force on the free-body diagram shown in figure 12 is

$$-\pi A_0^2 \rho \int_{D_2}^{D_1} r\,dr/r^2 = -\pi\rho A_0^2 \ln (D_2/D_1).$$

Conservation of vertical momentum implies that

$$-A_0^2 \ln (D_2/D_1) = D_2^2 W_2^2 - D_1^2 W_1^2, \tag{47}$$

or, after we define x and the Rossby number B as

$$x = D_2/D_1, \quad B = (2^{\frac{1}{2}} D_1 W_1)/A_0, \tag{48), (49}$$

(47), (48), (49) and (46) combine to yield

$$x - \{(2x \ln x)/B^2\} = 1/x \tag{50}$$

which is a transcendental equation for x in terms of the parameter B.

Consider the functions

$$y(x) = x - (2/B^2)\, x \ln x \quad \text{and} \quad z(x) = 1/x;$$

these functions are plotted in figure 13 on a log–log paper. The intersection of these curves yields two roots for x: x_1 and x_2. x_1 is always equal to unity, while x_2 moves on the arc $\alpha\beta$ when $B < 1$ and on the arc $\beta\gamma$ when $B > 1$. Values of $x < 1$ correspond to non-physical situations. Therefore, we must rule out the arc $\alpha\beta$. As in the hydraulic jump, the vortex breakdown occurs when the governing parameter is greater than unity or when the flow is supercritical. Here the Rossby

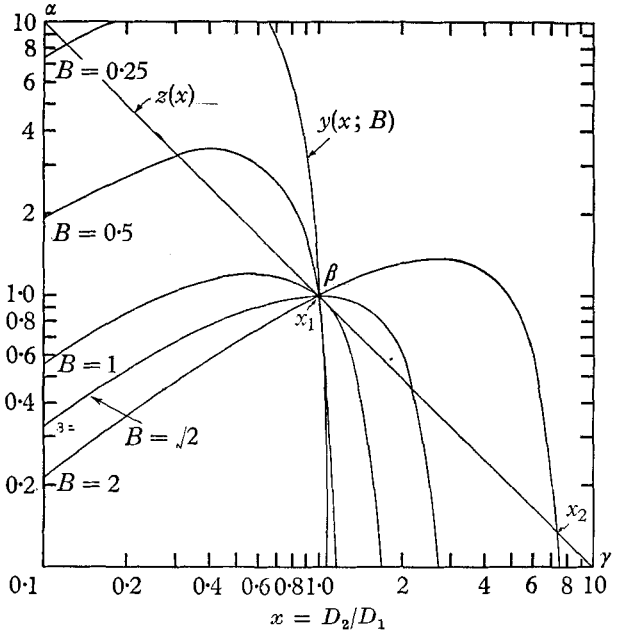

FIGURE 13. Plot of $y(x) = x - (2/B^2)x \ln x$ and of $z(x) = 1/x$ *vs*. x.

number plays the part of the Froude number in the hydraulic jump: from (49) we can estimate the Rossby number prevailing in the experimental flows; such a number varied between 2 and 2·5. As a result, x varied between 7 and 25; i.e. D_2 was predicted to be between 7 and 25 times bigger than D_1. These predictions agree with the experimental observations.

In the (**R**)-plane flow, the radius of the base of the axial core is $2{\cdot}5\epsilon^{\frac{1}{2}}$ and the plate boundary-layer flux at the origin is $-5{\cdot}7\epsilon^{\frac{1}{2}}$ so that the corresponding vertical velocity W_1 is

$$W_1 = 5{\cdot}7\epsilon^{\frac{1}{2}}/\pi(2{\cdot}5\epsilon^{\frac{1}{2}})^2$$

and

$$B = 2^{\frac{1}{2}}D(\epsilon)\,W_1 = \frac{2^{\frac{1}{2}}(2{\cdot}5\epsilon^{\frac{1}{2}})\,(5{\cdot}7\epsilon^{\frac{1}{2}})}{(2{\cdot}5\epsilon^{\frac{1}{2}})^2}$$

or

$$B = 1{\cdot}03.$$

The Rossby number is barely greater than critical.

9. Conclusions

In the decay of a vortex above a stationary boundary viscous forces play a major role in the set-up of a meridional circulation cell which carries mass, momentum and vorticity and which links all the various regions of the meridional plane. When diffusion of vorticity is the dominant mechanism for vorticity redistribution, we can arrive at an asymptotic solution of the plate boundary layer. A fluid particle when trapped in such a region remains in that layer and exits near the origin where the flow erupts into an axial boundary layer. The eruption shows that the flow in that region is essentially governed by an inviscid mechanism whereby large pressure gradients develop, slow down the plate boundary-layer flow and turn it into an axial flow. Very large vertical and swirl velocities are found in this region where the core radius is of order $\epsilon^{\frac{1}{2}}$. Centrifugal effects, by playing a role analogous to gravitational effects, can be responsible for the formation of a vortex breakdown which represents an abrupt transition from small to large core diameter. As a result, the whole axial boundary-layer structure is critically dependent on the flow conditions at its base. Along the axis, the problem is a difficult one due to the non-linearity of the flow and due to the variations of the radial pressure gradient across the axial layer. We have looked at the $O(\epsilon^{\frac{1}{2}})$ inviscid-flow solution but because of the lack of knowledge of the axial flow we were unable to link the different flow regions. This appeared in the solution as a set of unknown coefficients.

The author is indebted to Professor H. W. Emmons for suggesting the problem and for his encouragement and advice, to Professor D. Anderson for the numerous discussions and for his help in the numerical work connected with this problem, and to Professor G. Birkhoff for his assistance and advice. This work fulfilled part of the Doctoral requirements at Harvard University and was supported in part by the Office of Naval Research under Contract Nonr-1866(34) and by the Division of Engineering and Applied Physics, Harvard University.

REFERENCES

BARCILON, A. 1965*a* Secondary flow in a viscous vortex. Ph.D. Thesis, Harvard University.

BARCILON, A. 1965*b* Secondary flow in a viscous vortex. *Tech. Rept*, Department of Mathematics, Harvard University, Office of Naval Research Nonr-1866(34).

BENJAMIN, T. B. 1962 Theory of the vortex breakdown phenomenon. *J. Fluid Mech.* **14**, 593–629.

GOLDSTEIN, S. 1960 *Lectures on Fluid Mechanics*. London: Interscience.